A high-precision continuous-time positioning-navigation-timing (PNT) compact module for the LunaNet small spacecraft

2022 SmallSat Technology Partnerships (STP) Technology Exposition

NASA STP Technical Monitor: Rodolphe De Rosee
PI: Prof. Chee Wei Wong, UCLA
Co-I: Jaime Flor Flores, UCLA
NASA Center: Dr. A. Matsko, Dr. V. Iltchenko, and Dr. W. Zhang, JPL

STP 2020 Project: 80NSSC20M0082

June 8, 2022

Desired accelerometer performances for applications

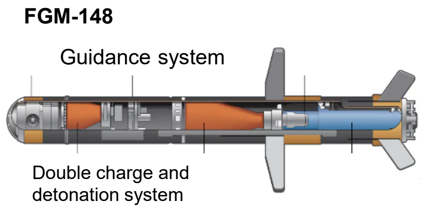

Smart Ammunition

Health Tracking

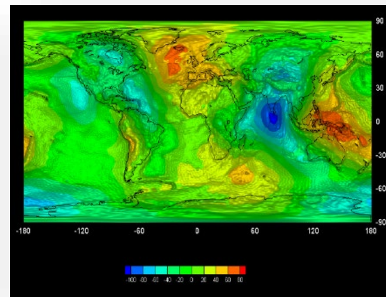

Gravimetry

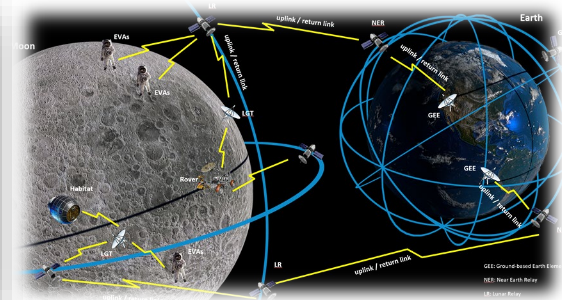

Inertial Navigation

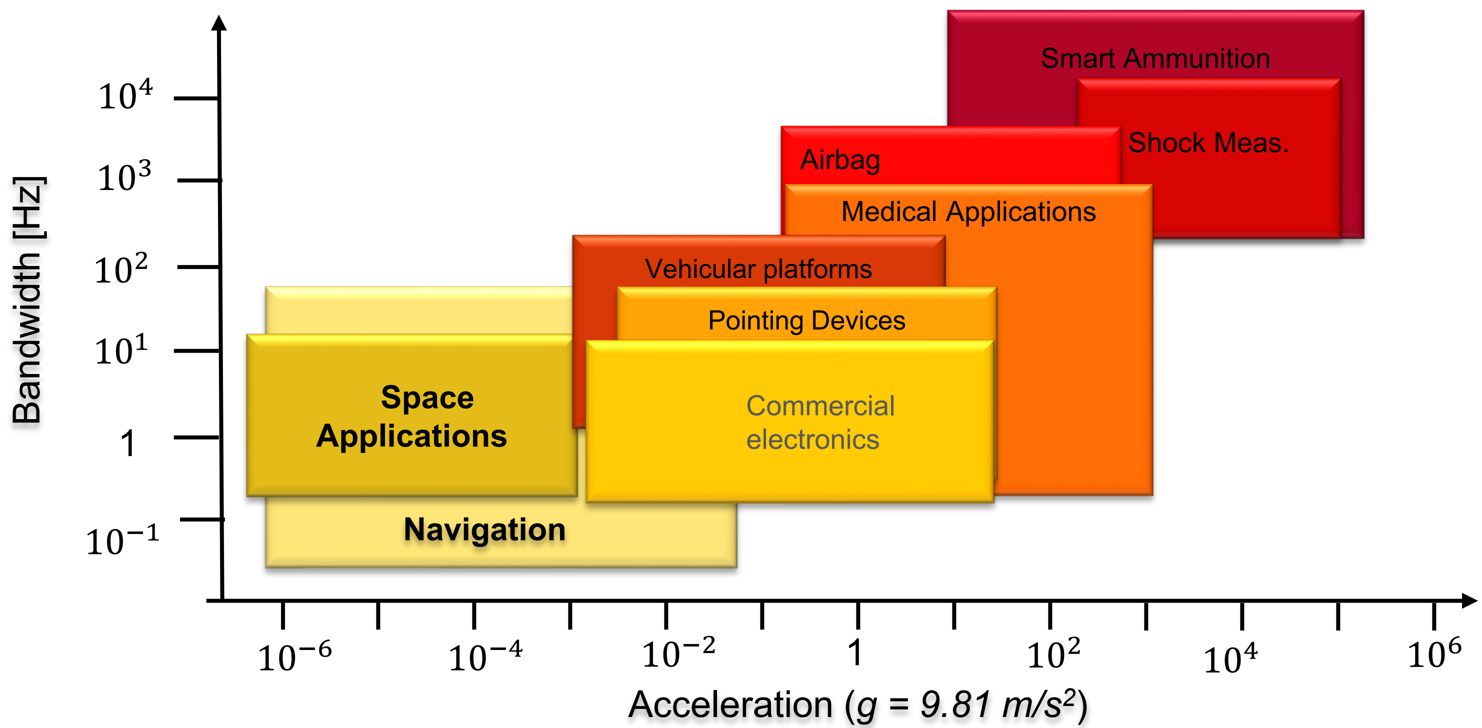

Source: Adapted from: Michael Kraft, *Micromachined inertial sensors state of the art and a look into the future.* Measurement and Control **33**. Others from Apptunix (2022).

Precision inertial navigation – performance metrics

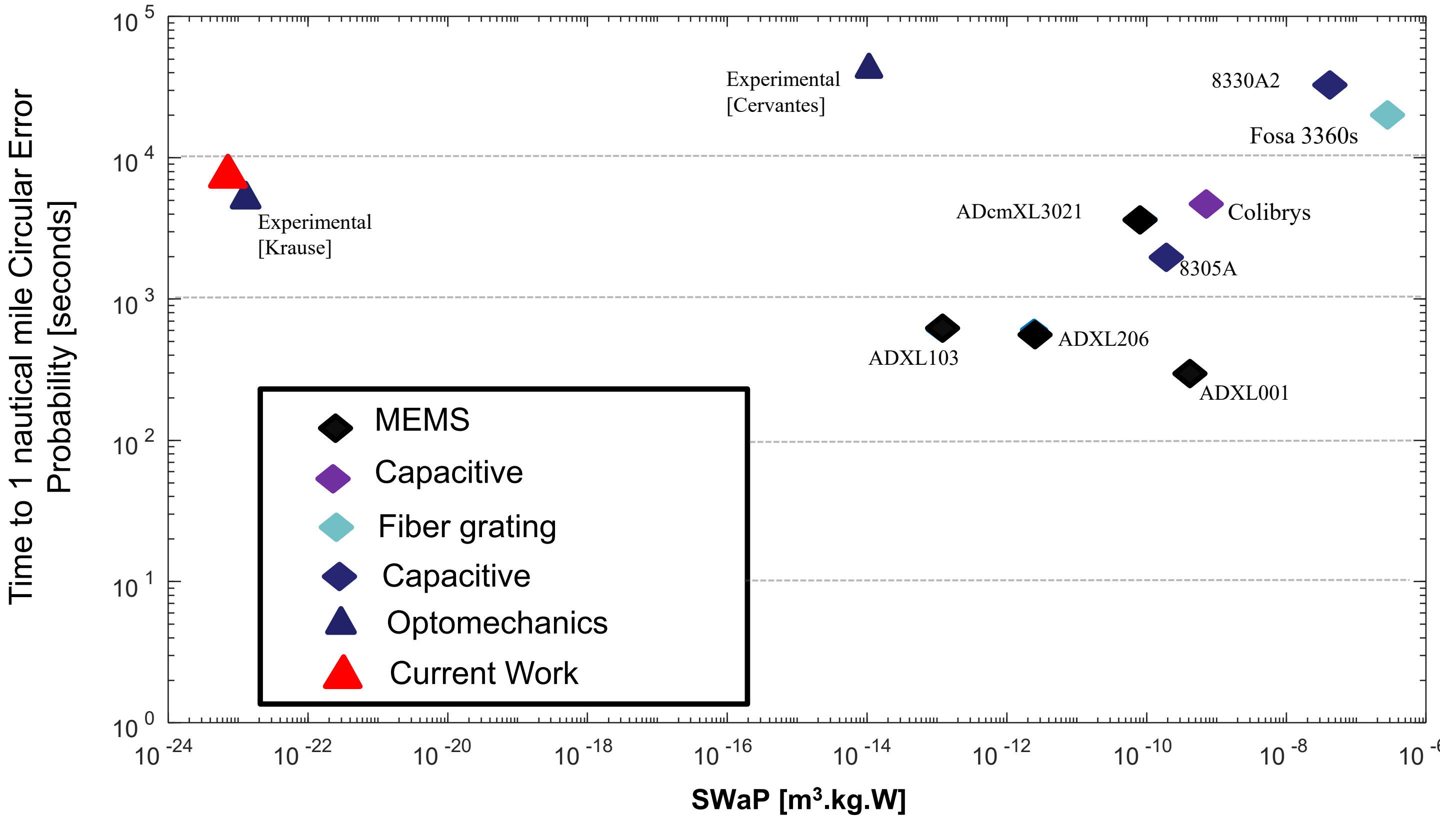

- **Size Weight and Power (SWaP).** SWaP vs. time to achieve a 1 nautical mile (nmi) error in seconds, for different accelerometers and technologies.
- Commercial accelerometers are shown and labeled by model and technology they use.
- Optomechanical accelerometers presented in red are our SSTP-STP device modules (pre-STP: bare chiplet lab demonstration).

Precision inertial navigation – detailed performance metrics

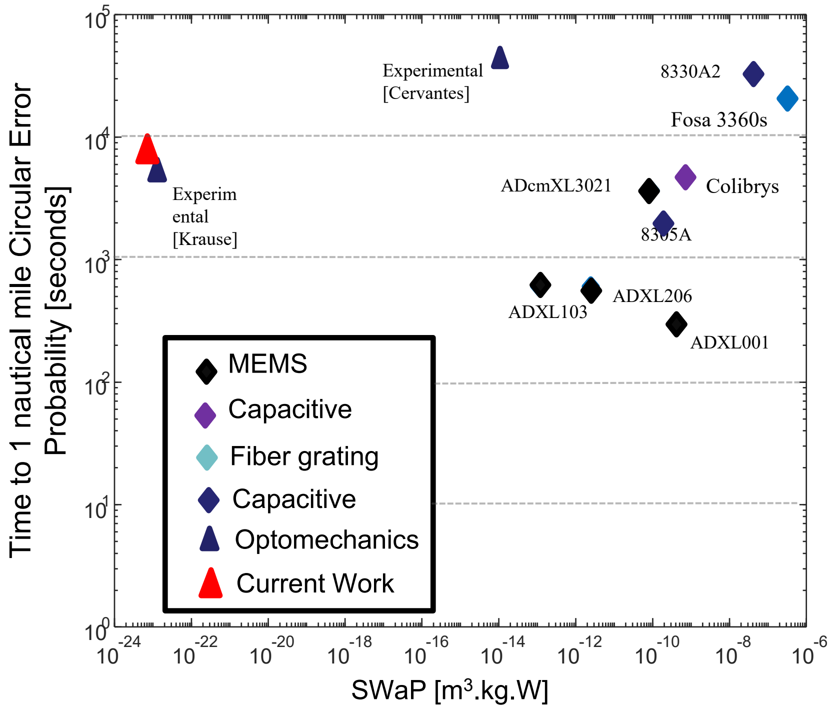

Via this 2020 STP program

Inertial sensor metric	Performance
Volume/Weight	full package 2.8 cm³ [chiplet is 0.034 cm³] 31.5 grams [chiplet is 0.08 grams]
Power	58 mW [1-2 W cont. operation of TEC]
Dynamic range	Future testing at 60 g
Velocity random walk	8 µg/Hz$^{1/2}$
Bias sensitivity	1.3 mg/Hz
Scale factor repeatability	optical resonance repeatability at ~0.7 ppm
Bias instability	52 µg

- Demonstrated metrics of the chip-scale inertial sensor, in support of the LunaNet PNT technology mission

Packaged inertial navigation unit with significant experience from JPL

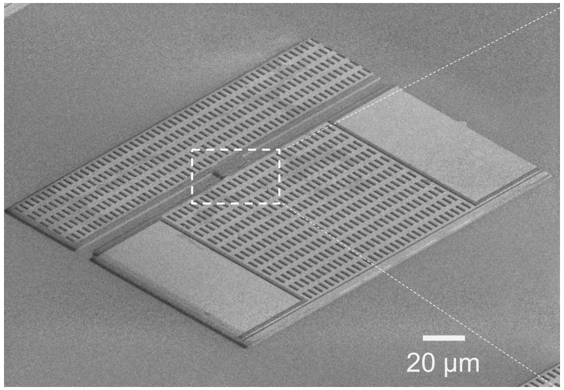

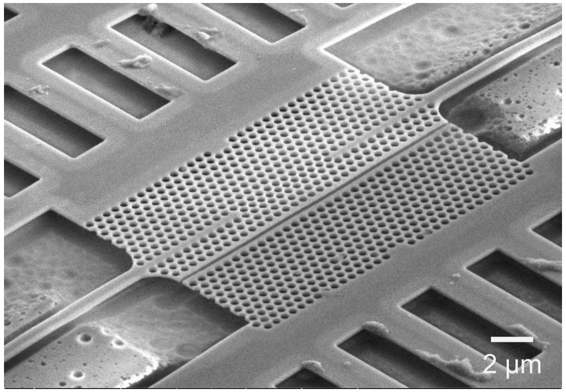

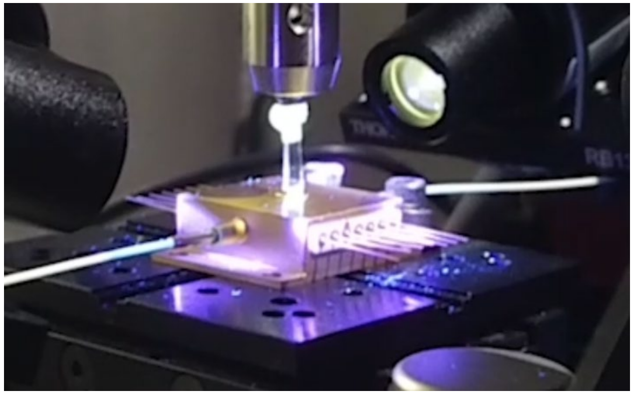

Inertial navigation – fundamental operating architecture

1. Light forces at the Nanoscale

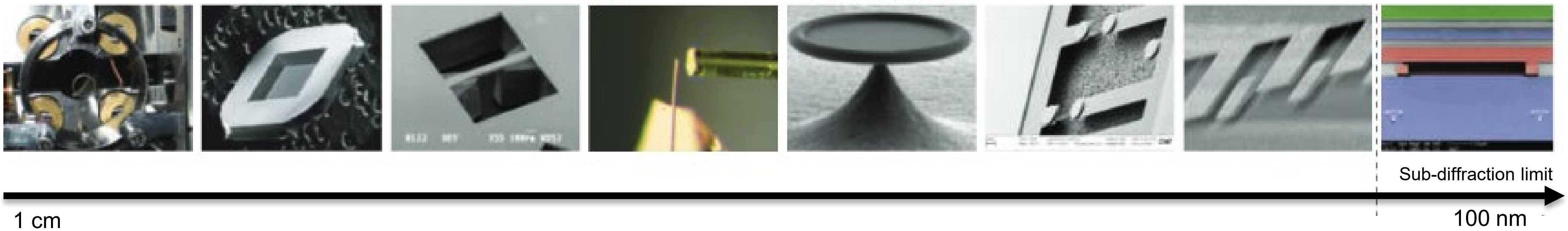

2. Coupled mode and first-order perturbation theory

$$\frac{da}{dt} = i\Delta(x)a - \left(\frac{1}{2\tau_0} + \frac{1}{2\tau_{ex}}\right)a + i\sqrt{\frac{1}{2\tau_{ex}}}s \qquad \Delta(x) = \Delta + g_{OM}x = (\omega - \omega_o) + g_{OM}x$$

$$\frac{d^2x}{dt^2} + \frac{\Omega_m}{2Q_m}\frac{dx}{dt} + \Omega_m^2 x = \frac{F_o}{m_{eff}} + \frac{F_{th}}{m_{eff}} = -\frac{|a|^2 g_{OM}}{m_{eff}\omega_0} + \frac{F_{th}}{m_{eff}}$$

3. Optomechanical coupling

$$g_{om} = \frac{d\omega}{dx} \qquad L_{om}^{-1} = \frac{1}{\omega}\frac{d\omega}{dx}$$

4. First-order perturbation theory

$$g_{om} = \frac{1}{2\omega}\frac{\int dA\left(\vec{q}\cdot\hat{\vec{n}}\right)\left[\Delta\varepsilon|E|^2 - \Delta\left(\varepsilon^{-1}\right)|D|^2\right]}{\int dV\varepsilon\,|E(r)|^2}$$

- H. A. Haus, *Waves and Fields in Optoelectronics*.
- S. G. Johnnson et al. *Phys. Rev. E* **65**,066611 (2002).
- C. W. Wong et al. *Appl. Phys. Lett.* **84**, 1242 (2004).
- M. Eichenfield et al. *Optics Express* **17**, 20078 (2009).

Cavity optomechanics: optimized slot-cavity nanofabrication

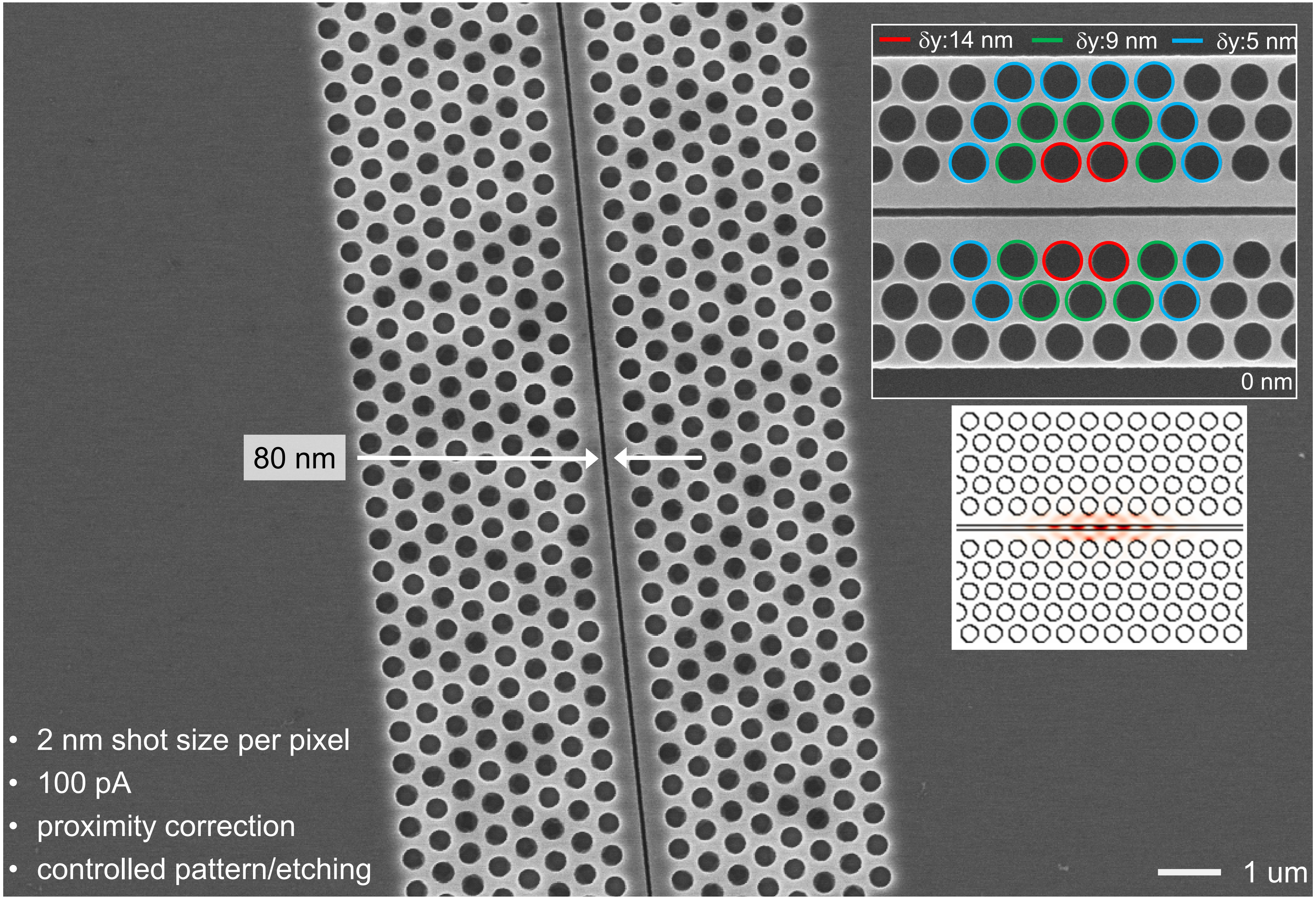

- 2 nm shot size per pixel
- 100 pA
- proximity correction
- controlled pattern/etching

D. Wang and M. Dadgar (Wong) et al.

Inertial accelerometer: optical & mechanical design

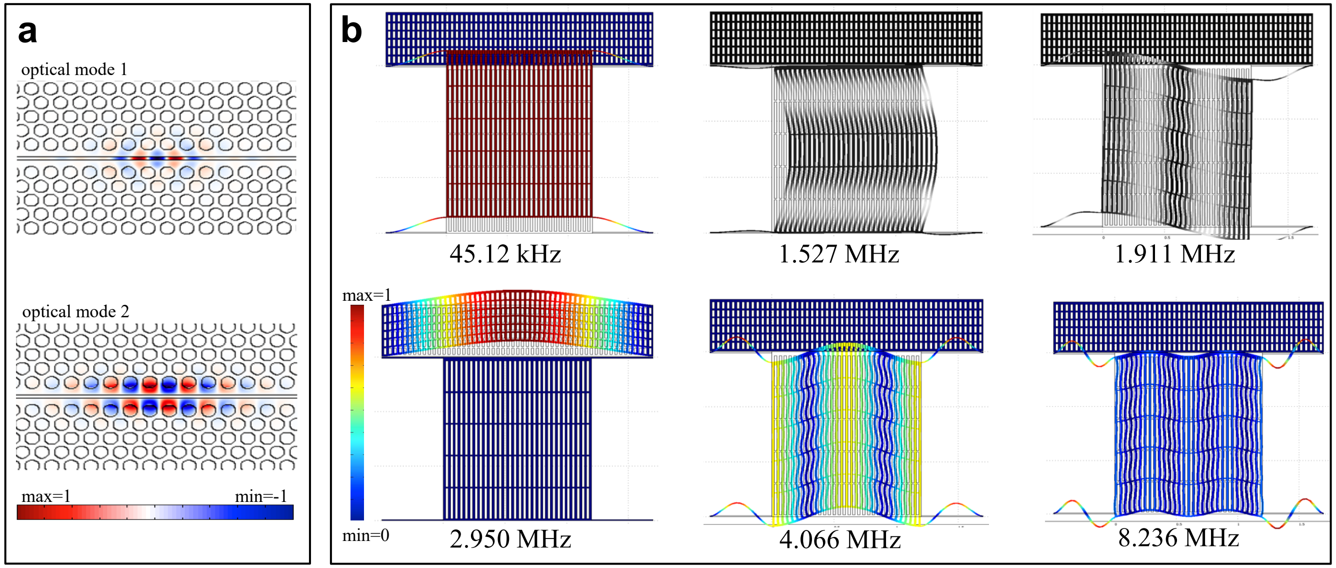

- **Mechanical modes** designed for the oscillation-mode accelerometer.
- Fundamental mode at 45.12 kHz.
- forbidden modes in grey. These modes are not allowed due to symmetry constrains.
- finite-element modeling.

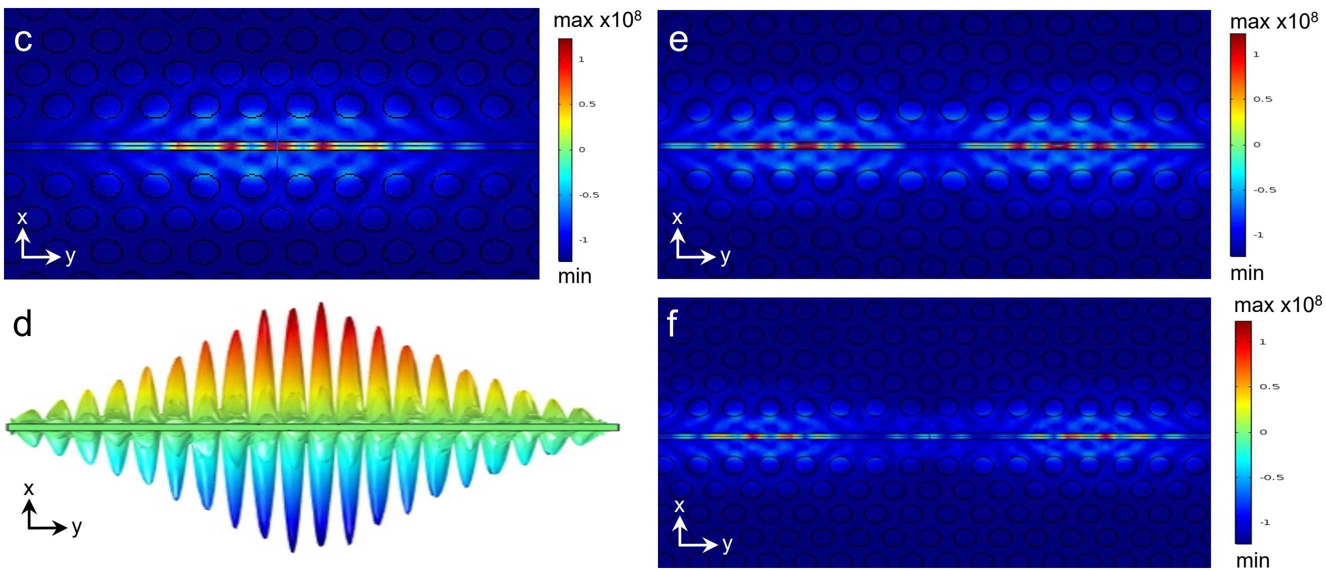

- **Simulated optical modes.** Figures c-f represent the calculated electric field $(V/m)^2$ of the optical mode for the fully integrated photonic crystal
- **c.** Fundamental mode
- **d.** x-z view of the zoomed in z-component electric field (V/m)
- **e.** Second-order mode.
- **f.** Third-order mode.

- Q_{theory} ~ 4,000,000 (Q_{expt} ~ 200,000)
- mode volume V ~ $0.02(\lambda/n_{air})^3$

Inertial optomechanical oscillator: high dynamic range and precision force sensing

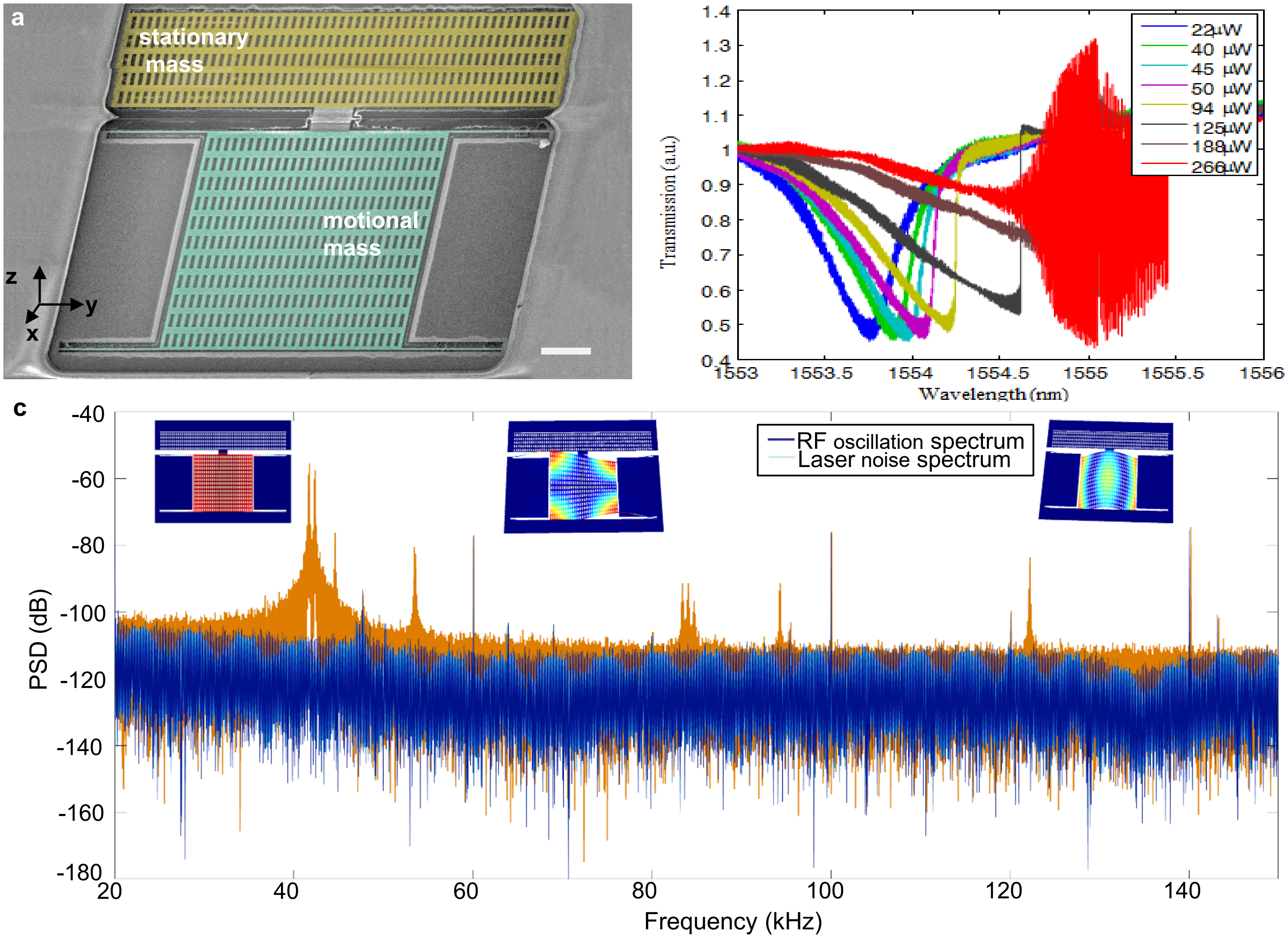

- RF mode of the optomechanical accelerometer with integrated waveguides
- Transmission spectra is monitored for cavity coupling, the main measurements are done in parallel by RF optical readout.

Inertial acceleration signal detection

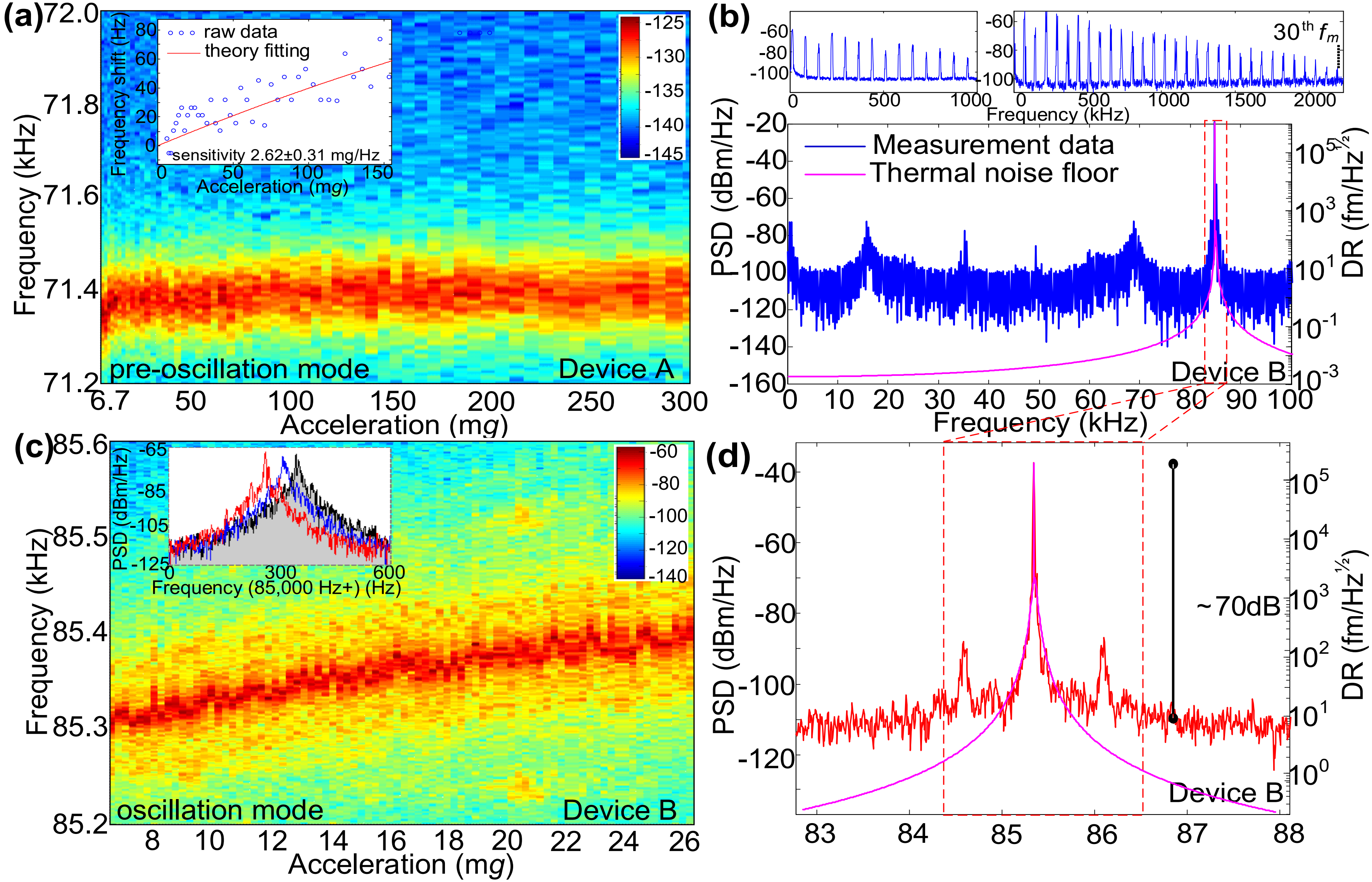

Y. Huang, J. G. Flor Flores, Y. Li, W. Wang, D. Wang, N. Goldberg, J. Zheng et al., A chip-scale oscillation-mode optomechanical inertial sensor near the thermodynamical limits, *Laser & Photonics Reviews* **14**, 1800329 (2020).

Oscillation and pre-oscillation modes performance

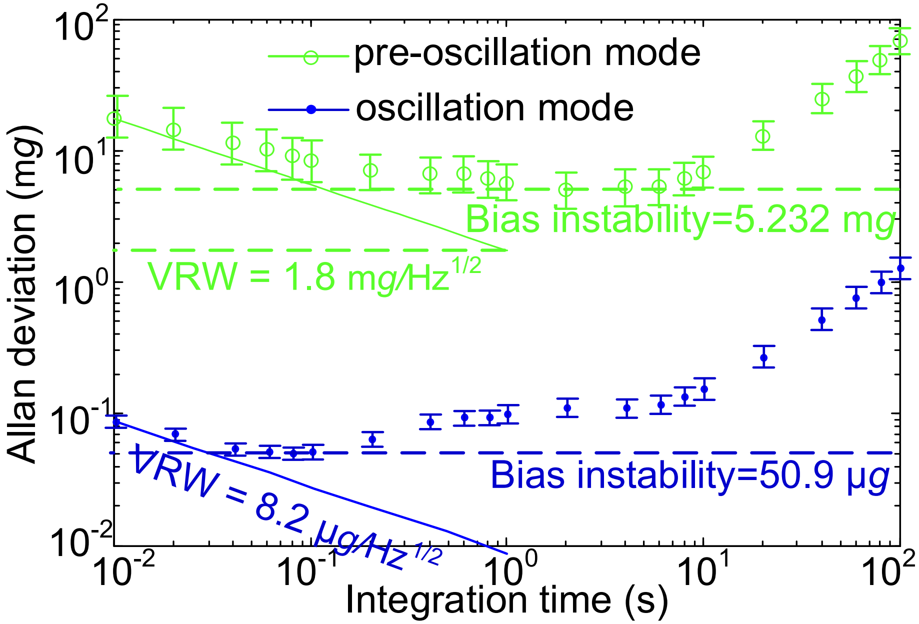

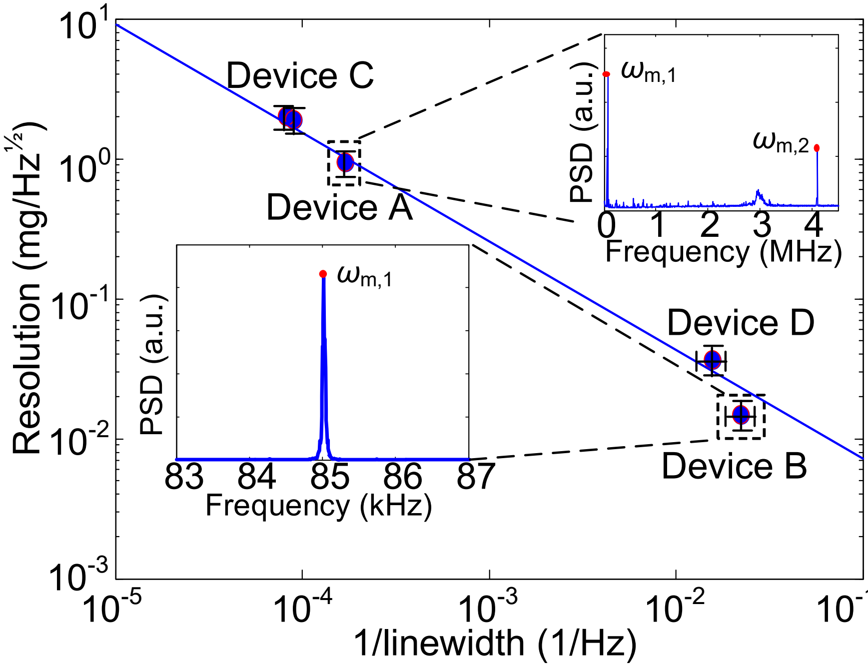

- Allan deviation measured at the pre-oscillation and oscillation modes.
- 220× Improvement in the oscillation mode compare to pre-oscillation.
- optomechanical coupling rate of 37.1 GHz/nm.
- further stability can be improved with laser stabilization.

Y. Huang, J. G. Flor Flores, Y. Li, W. Wang, D. Wang, N. Goldberg, J. Zheng et al., A chip-scale oscillation-mode optomechanical inertial sensor near the thermodynamical limits, *Laser & Photonics Reviews* **14**, 1800329 (2020).

Inertial accelerometer noise sources: kT, backaction and relative intensity noise

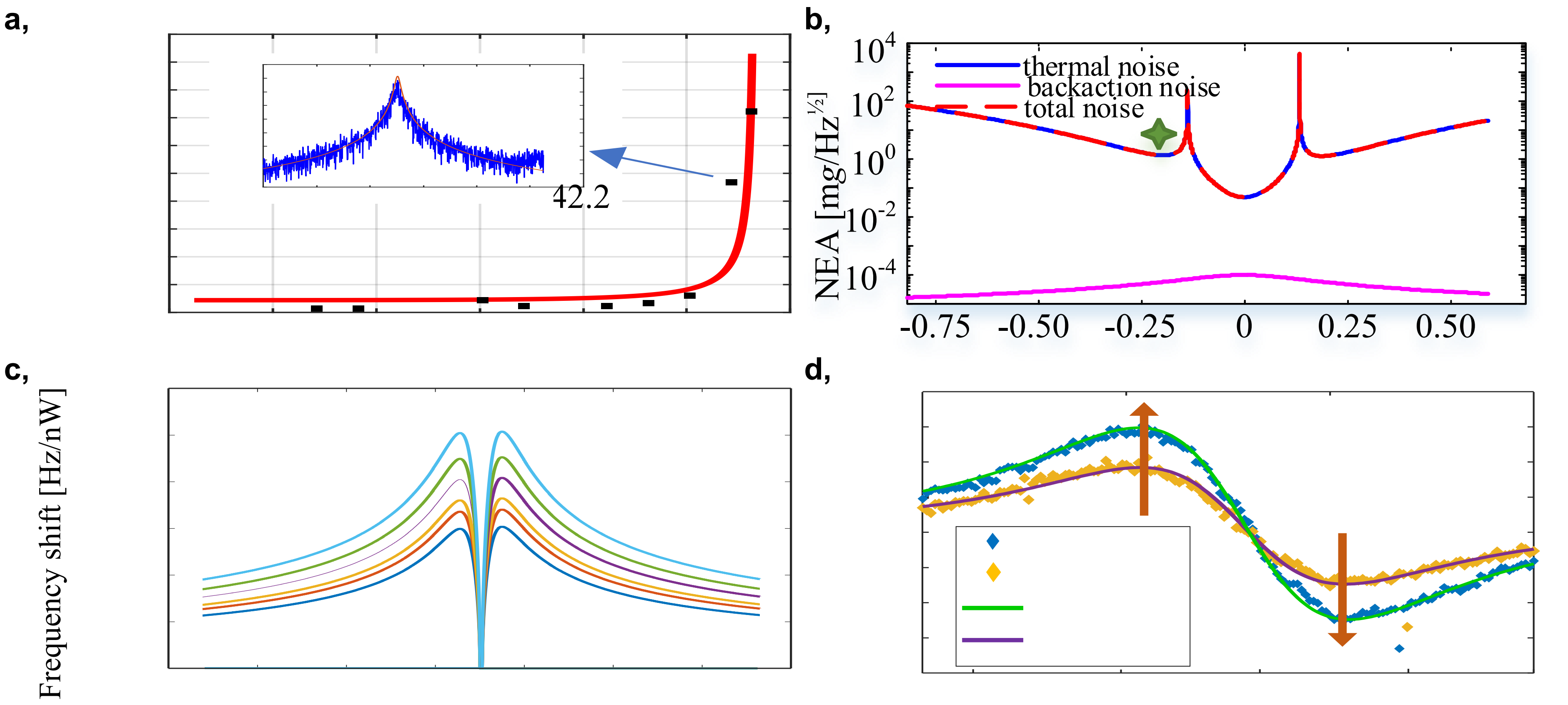

- theoretical limit includes thermal (kT) noise components as well as backaction noise.
- measurement noise sources such as laser intensity noise can be accounted for inertial navigation system.
- estimated maximum sensitivity to laser intensity noise is 0.2 Hz/nW at maximal inertial motion. Smaller displacements present smaller noise contributions.

Precision inertial accelerometer: package design

1. 3D view of the optomechanical inertial accelerometer (OMI) package design

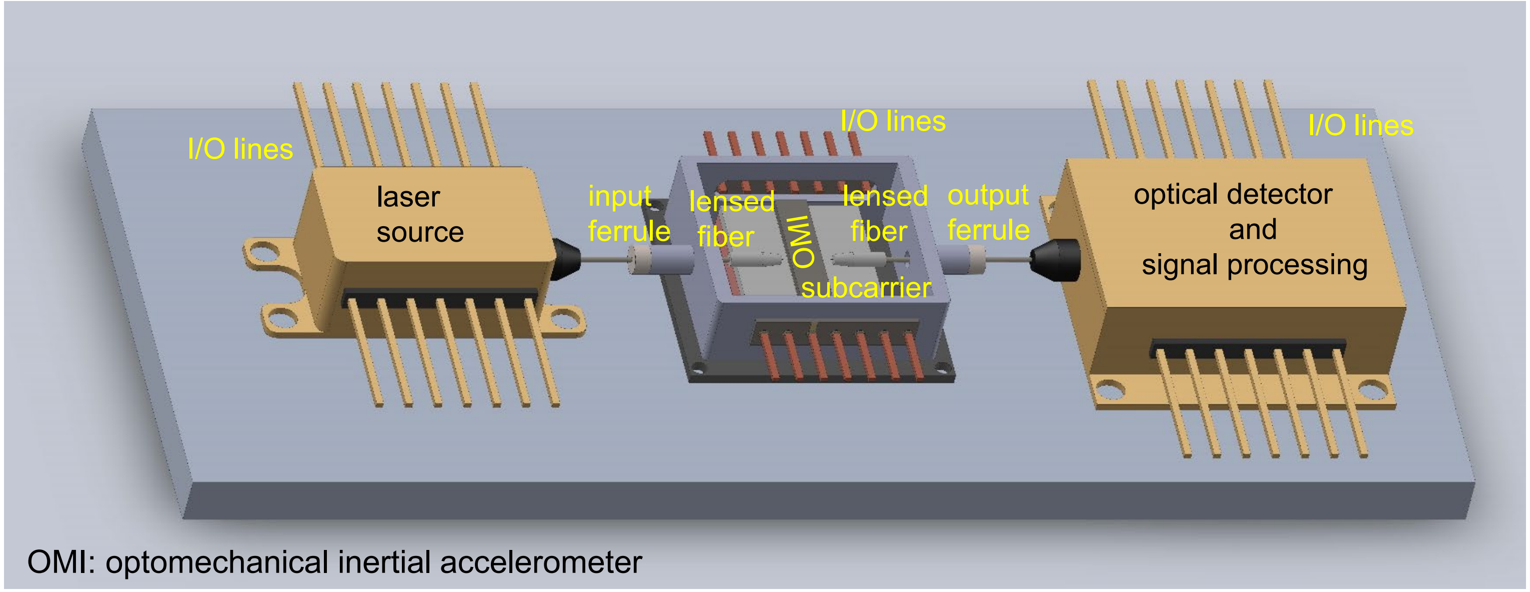

2. OMI integration and design

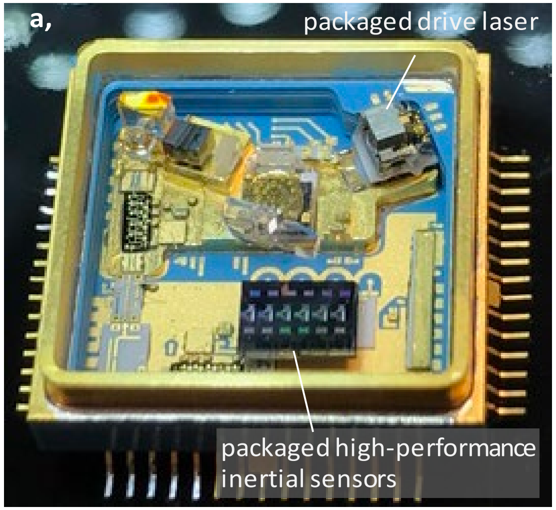

3. Integrated optomechanical transducer with on-chip detector

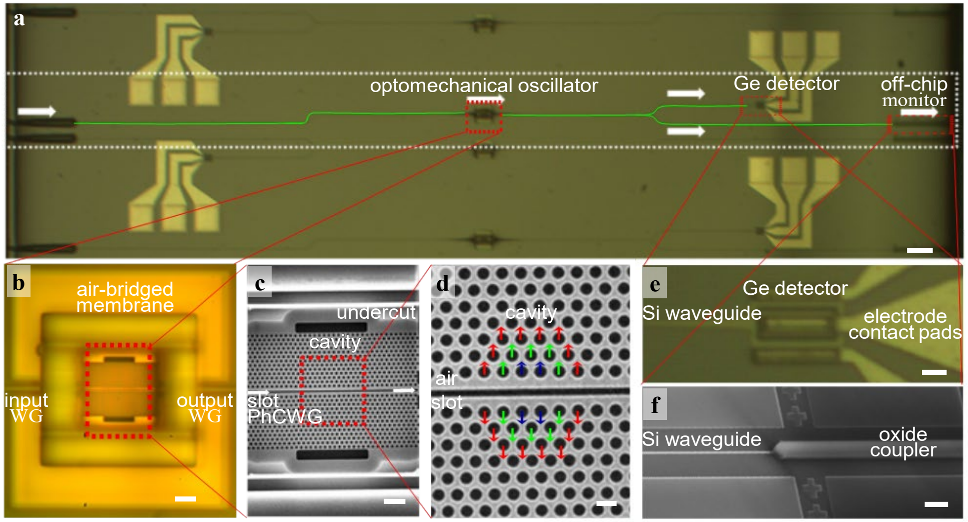

Precision inertial accelerometer: packaging tests

- 3D view of the accelerometer package design components
- guided by JPL rich experience

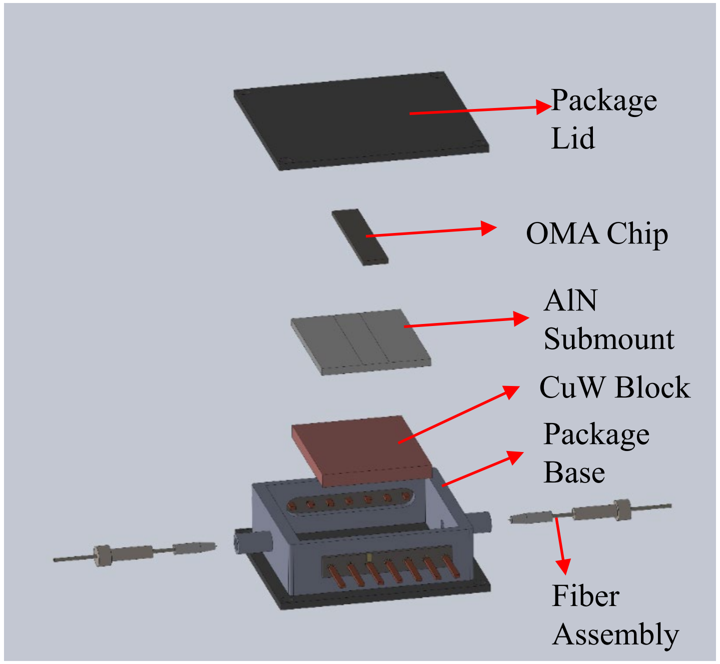

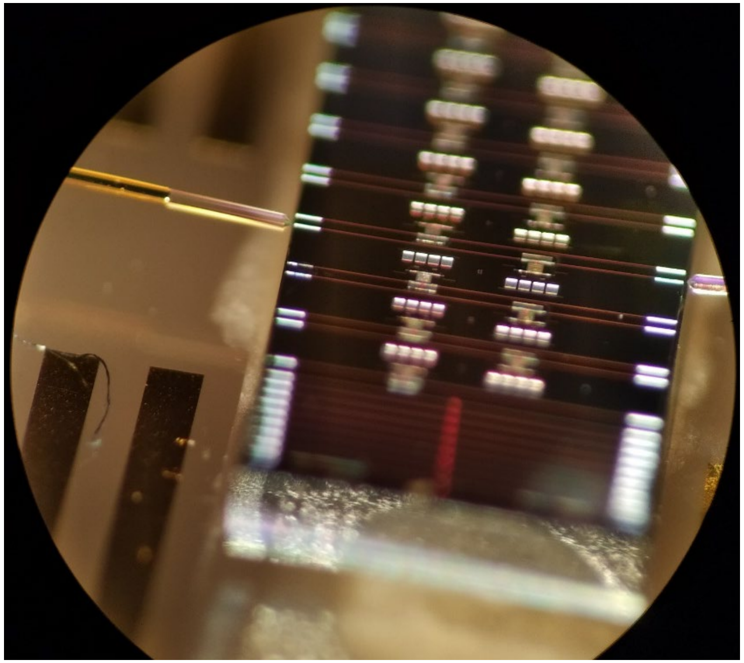

- laser-drive power and detectors are coupled by tapered lensed fibers.
- triple-stage inverse couplers and waveguides on-chip implemented for coupling to photonic crystal cavity sensor.
- accelerometer package optimized for thermal expansion coefficient matching
    - AIN subcarrier provides a coupling interface between the butterfly package and the Si chiplet.
    - CuW block for enhanced heat transfer.
    - hermetic package.
    - active alignment is externally controlled.
    - external TEC.

Hermetic UV sealing

Details of active alignment packaging process

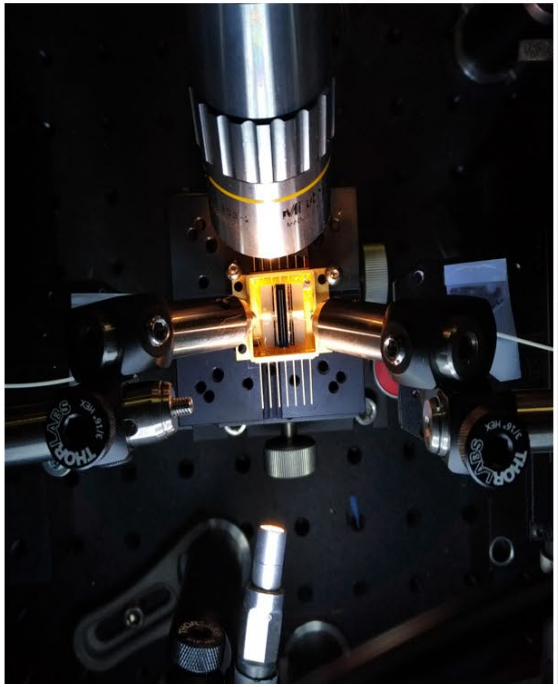

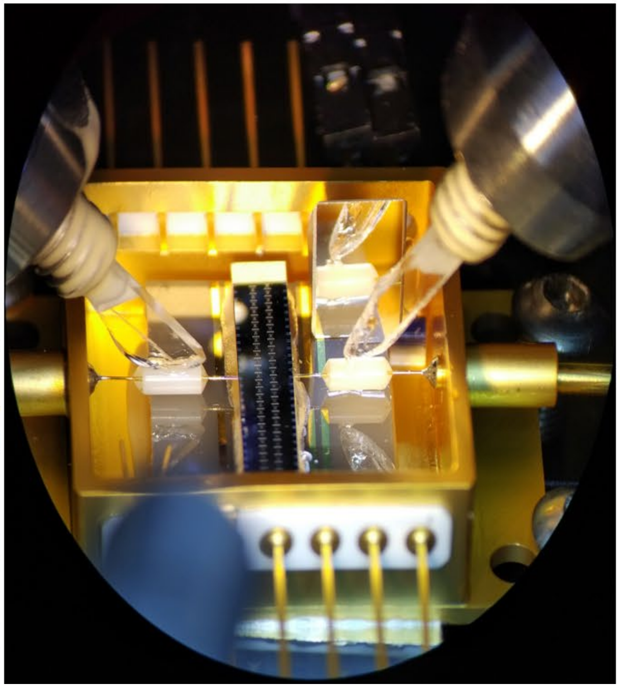

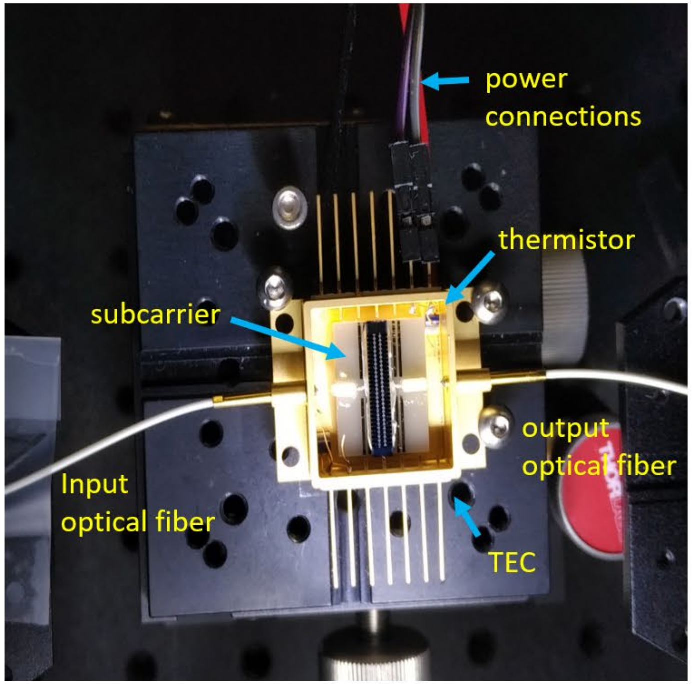

- active alignment setup to couple custom-made lensed fibers to the on-chip inverse couplers.
- optical fiber bonding process during optical active alignment
- optomechanical inertial accelerometer after active alignment and support mechanism released: laser coupling to chip maintained and stabilized.

- **Microscope image of nanofabricated optomechanical inertial sensor packaged at UCLA**
  - active alignment on 6-axis system.
  - optimized multiple epoxies for controlled adhesive bonding to minimize optical power loss.
  - images describe the fiber active alignment process as the adhesive is cured for and the tapred optical fibers held in place.
- **Ni-Co butterfly package with hermetic sealing**

Frequency Counting: frequency-to-voltage approach

a, Designed circuit block

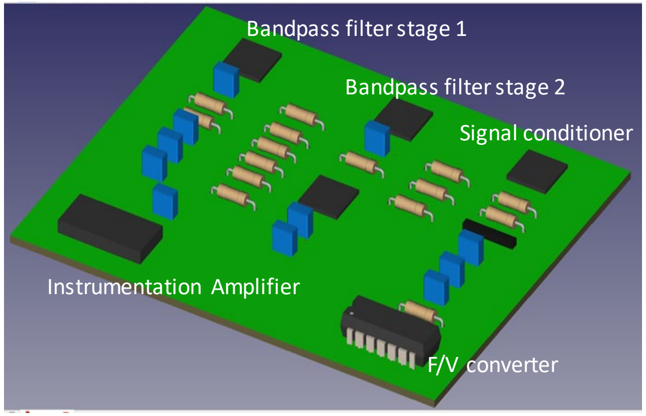

- **Optomechanical Inertial accelerometer readout circuits & drivers**
  - Instrumentation amplifier
  - 2 stage bandpass filter
  - Signal conditioner
  - Frequency to voltage converter
  - Connected to main processing unit
- **Breadboard and PCB implementation.**
  - compact size for final integration with OMA

b, Initial testing, and anticipated frequency resolution of inertial accelerometer readout

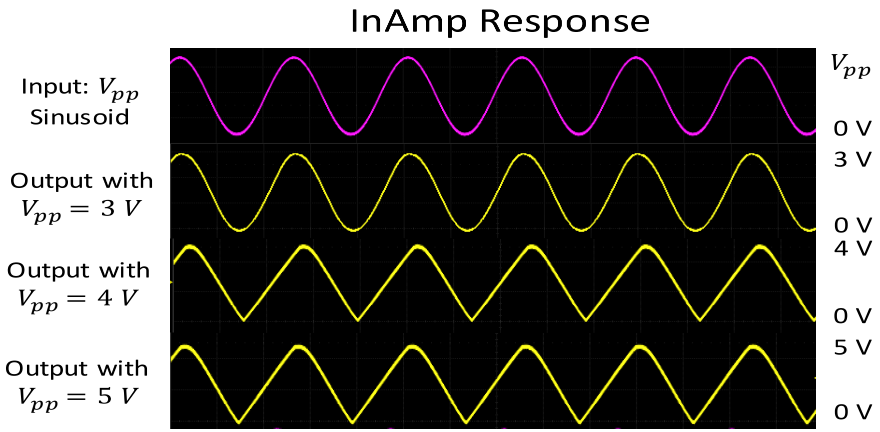

Reference	Resolution
1 MHz	10 Hz
10 MHz	1 Hz
100 MHz	100 mHz
1 GHz	10 mHz
10 GHz	1 mHz

Floor planning of subsystem boards with 3U CubeSat housing

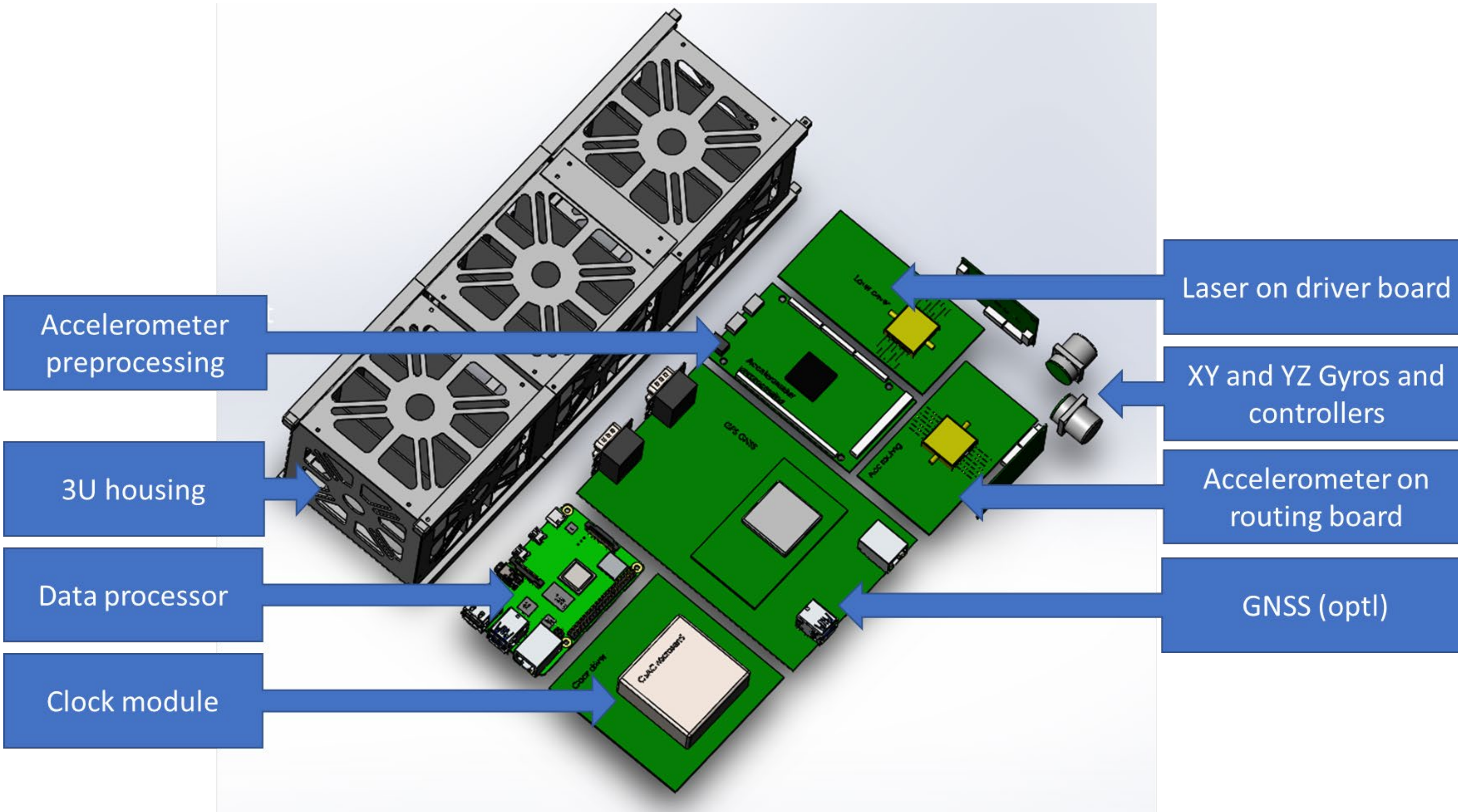

A high-precision continuous-time positioning-navigation-timing (PNT) compact module for the LunaNet small spacecraft

2022 SmallSat Technology Partnerships (STP) Technology Exposition

NASA STP Technical Monitor: Rodolphe De Rosee
PI: Prof. Chee Wei Wong, UCLA
Co-I: Jaime Flor Flores, UCLA
NASA Center: Dr. A. Matsko, Dr. V. Ilchenko, and Dr. W. Zhang, JPL

STP 2020 Project: 80NSSC20M0082